

# Role of quantum capacitance in coupled low-dimensional electron systems

M. Ruß, C. Meier, and A. Lorke\*

*Experimental Physics, University of Duisburg-Essen, Lotharstraße 1, D-47048 Duisburg, Germany*

D. Reuter and A. D. Wieck

*Lehrstuhl für Angewandte Festkörperphysik, Ruhr-Universität Bochum, Universitätsstraße 150, D-44780 Bochum, Germany*

(Received 9 December 2005; revised manuscript received 16 February 2006; published 27 March 2006)

We have investigated the charging behavior of a layer of self-assembled InAs quantum dots placed in close vicinity to a two-dimensional electron gas (2DEG). As the gate bias is changed, the number of electrons in each system is altered simultaneously. Based on the quantum capacitance of the involved layers we develop a general model to determine the charging state of coupled low-dimensional systems from capacitance-voltage (CV) spectroscopy. The model is then applied to the special case of a layer of self-assembled quantum dots coupled to a 2DEG. As a complementary method, we have employed Hall voltage measurements. We find that the measurement of the two-dimensional carrier density through lateral transport provides a direct insight into the vertical charging process of the quantum dot system. Six individual charging peaks related to the occupation of the  $s$  and  $p$  shells of the dots can be resolved. In agreement with results from CV spectroscopy, Coulomb blockade and quantization energies can be extracted. Moreover, the Hall measurement offers a higher peak-to-valley ratio and a better estimate for the number of simultaneously charged dots than the capacitance data.

DOI: [10.1103/PhysRevB.73.115334](https://doi.org/10.1103/PhysRevB.73.115334)

PACS number(s): 73.21.La, 73.22.-f, 73.23.Hk

## I. INTRODUCTION

Self-assembled quantum dots (SAQDs) have attracted much interest due to the fact that they show full quantization for electrons and holes with atomlike properties.<sup>1-3</sup> For the investigation of the internal electronic structure, capacitance-voltage (CV) spectroscopy has proven to be a valuable tool. In most cases, a three-dimensional (3D) electron reservoir is used and the ac tunneling current between the dots (0D system) and the 3D reservoir is monitored.<sup>4-7</sup> Measured changes in capacity are directly linked to the electronic density of states of the quantum dots. This way the charge per quantum dot can be determined very precisely.

However, for a number of experiments it is of interest to rather use a two-dimensional electron gas (2DEG) as a reservoir. For example it has been demonstrated that SAQDs in close vicinity of a 2DEG can greatly affect the scattering times and thus the mobility of the 2DEG.<sup>8</sup> Also, several authors have demonstrated that the properties of a 2DEG in the quantum Hall regime can be directly influenced by a nearby quantum dot layer.<sup>9-13</sup>

A major difficulty in these experiments is the uncertainty of the exact charge states of the 2D and 0D systems. This is due to the fact that a change in applied gate voltage affects both carrier densities simultaneously and the calculation of, e.g., the resulting mobility of the 2DEG is directly based on both quantities. Therefore, an exact knowledge of the individual charging states is necessary in order to analyze the 2D-0D interaction properly.

In this paper we use two complementary methods to detect the respective charge densities: CV spectroscopy and Hall measurements. Surprisingly, also the in-plane Hall measurements allow for a detection of the vertical tunneling events into the quantum dot layer. We develop a general model of layered quantum systems and apply it to accurately

determine the charging state of the QD layer. While both techniques deliver accurate results for the electron densities, the spectroscopic resolution of the Hall measurements is superior to that of CV measurements. Moreover, it allows spectroscopy for almost arbitrarily slow time scales and therefore gives access to a regime where ac-based experiments are no longer practical.

## II. SAMPLES AND EXPERIMENTAL SETUP

The general structure of our samples is very similar to metal-insulator-semiconductor field-effect transistor structures with a 3D reservoir used in earlier work.<sup>5,6,14,15</sup> The main difference of our samples is the two-dimensional electron gas used as a back contact.

All samples were grown by solid-source molecular-beam epitaxy on GaAs (100) semi-insulating substrates. First, a GaAs buffer was deposited, followed by 150 nm  $\text{Al}_{0.34}\text{Ga}_{0.66}\text{As}$ , a Si- $\delta$ -doping layer, and a 40 nm  $\text{Al}_{0.34}\text{Ga}_{0.66}\text{As}$  spacer. Then, the 40 nm thick GaAs tunneling barrier was grown, followed by the InAs quantum dots. On top of the dots, 30 nm of GaAs and a 200 nm thick AlAs/GaAs superlattice were grown, preventing tunneling to the sample surface. Finally, the structure was capped with 10 nm GaAs and a second layer of InAs was deposited on the sample surface. From atomic force micrographs of these surface dots we estimate the dot density to be approximately  $7 \times 10^9 \text{ cm}^{-2}$ . In this structure the 2DEG is formed at the interface between the 40 nm  $\text{Al}_{0.34}\text{Ga}_{0.66}\text{As}$  spacer and the 40 nm GaAs tunneling barrier, as depicted in Fig. 1. The mobility of the 2DEG is about  $9 \text{ m}^2/\text{V s}$  at  $n_{2D}=3.8 \times 10^{15} \text{ m}^{-2}$ .

We have prepared Hall bar devices with a metallic top gate in order to control the charge state of the device. Addi-

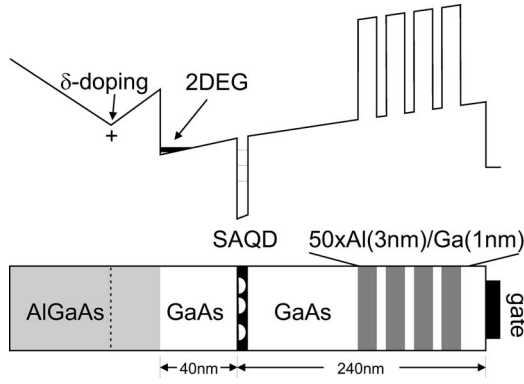


FIG. 1. Sketch of the conduction band and layer sequence of the heterostructure. The GaAs tunneling barrier between the 2D back contact and the quantum dot layer is transparent in the frequency range employed for CV and Hall measurements. The superlattice prevents leakage to the gate electrode. A capacitance maximum is observed when tunneling from the Fermi level of the 2D gas into the discrete energy levels of the quantum dots is possible.

tionally, large area gates have been prepared on the same samples. All electrical measurements have been performed in a He cryostat at  $T=4.2$  K in the low-frequency lock-in technique. In the Hall experiments, an external magnetic field of  $B=0.3$  T has been applied perpendicular to the sample surface. At this magnetic field Hall plateaus just begin to emerge, but their effect is small compared to the main features observed in our experiments.

### III. MODEL

In the following we derive an iterative model to describe the charging state of a gated heterostructure with an arbitrary number of embedded quantum systems with a reduced (non-metallic) density of states. This model is then applied to our specific sample geometry. The main aim of the calculation is to perform a detailed analysis of capacitance data. However, the derived equations also enable us to use lateral Hall measurements of the 2DEG to determine the number of electrons tunneling vertically into the SAQD.

The following analysis is directly related to the field penetration method, which was previously used to determine the density of states of two-dimensional electron gases.<sup>16,17</sup> Here, we extend this model to an arbitrary number of embedded quantum systems that interact via fast tunneling processes. Because of this tunnel coupling we can use an iterative formalism to calculate the resulting capacitance, where each step resembles the simple situation discussed by Luryi.<sup>18</sup> This way, we avoid the complications that arise when the capacitance of a system with a number of *individual* mesoscopic systems coupled to different reservoirs is calculated. A general model for the capacitance of such an arbitrary number of interacting conductors was developed by Büttiker.<sup>19</sup>

To iteratively solve the problem of a layered system as shown in Fig. 1, we start from an empty capacitor<sup>27</sup>  $C^{(0)}$ , which consists of a metallic gate electrode and a back electrode. The back electrode is at present not further specified

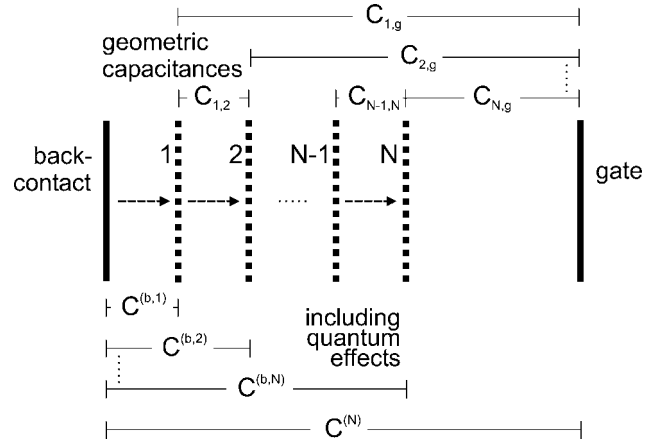


FIG. 2. Model of a sample with  $N$  embedded quantum systems in thermal equilibrium with an arbitrary back electrode.  $C_{i,j}$  denotes the purely geometric capacitance between two layers, while quantum effects enter the values for  $C^{(b,i)}$ , corresponding to the total capacitance between the back contact and layer  $i$ .  $C^{(N)}$  is the total resulting capacitance of the sample after  $N$  quantum systems have been included in the iteration. The arrows indicate which are electrically connected through a tunneling barrier.

and can in fact be of complex nature (see below). In the first step, we insert a (quantum) layer 1 into the capacitor (see Fig. 2). This layer is electrically connected (usually by a tunneling barrier) to the back electrode, but insulated from the gate electrode.

In order to obtain the resulting capacitance of this new system  $C^{(1)}$ , we write the differential change in voltage  $dU$  across the structure as

$$dU = \frac{d\sigma_g}{C_{1,g}} + \frac{d\sigma_1}{e^2 D_1}. \quad (1)$$

Here, the first term on the right-hand side accounts for the change in electrical potential, which is given through Gauss' law by the change in charge on the metallic gate,  $d\sigma_g$ . The second term results from the change in chemical potential in layer 1, given by the charge  $\sigma_1$  and the density of states  $D_1$ . The position of the inserted layer is expressed in terms of the geometric capacitance  $C_{1,g}$  between gate and layer 1, which also contains the effective dielectric constant of the medium between these layers.

Similarly, the fact that the back contact and layer 1 are in equilibrium yields

$$0 = \frac{-d\sigma_{b,1}}{C^{(b,1)}} + \frac{d\sigma_1}{e^2 D_1}, \quad (2)$$

where  $\sigma_{b,1}$  is the change in charge on the back electrode. Note that any change in the chemical potential in the back electrode is already accounted for by the effective capacitance  $C^{(b,1)}$ . Since  $1/C^{(0)}$  is a serial composition of  $C_{1,g}$  and  $C^{(b,1)}$ , it is given by

$$\frac{1}{C^{(b,1)}} = \frac{1}{C^{(0)}} - \frac{1}{C_{1,g}}. \quad (3)$$

From Eqs. (1)–(3) and charge conservation

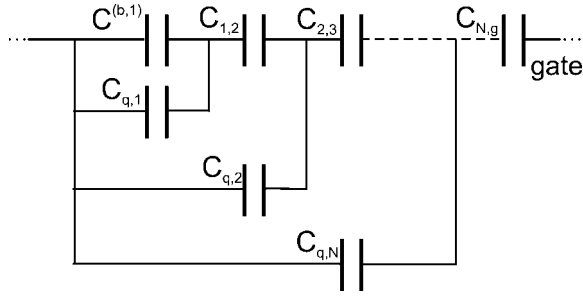


FIG. 3. Capacitance network corresponding to the iterative formalism [Eqs. (6) and (8)]. The quantum capacitance of the  $i$ th system appears in parallel to all systems with an index  $k < i$ .

$$-d\sigma_g = d\sigma_{b,1} + d\sigma_1, \quad (4)$$

the capacitance  $C^{(1)} = d\sigma_g/dU$  follows

$$\frac{1}{C^{(1)}} = \frac{1}{C_{1,g}} + \frac{1}{C_{q,1} + C^{(b,1)}}, \quad (5)$$

with the quantum capacitance<sup>18</sup>  $C_{q,1} = e^2 D_1$ . Since  $C^{(1)}$  can also be viewed as a capacitance resulting from a metallic gate electrode and a complex back electrode, Eq. (5) can be iterated and the capacitance of a layered system follows from the iterative equations

$$\frac{1}{C^{(i)}} = \frac{1}{C_{i,g}} + \frac{1}{C_{q,i} + C^{(b,i)}}, \quad (6)$$

$$\frac{1}{C^{(b,i)}} = \frac{1}{C^{(i-1)}} - \frac{1}{C_{i,g}} \quad (7)$$

$$= \frac{1}{C_{i-1,i}} + \frac{1}{C_{q,i-1} + C^{(b,i-1)}}. \quad (8)$$

Again, all systems  $1, \dots, i$  are assumed to be in equilibrium with the back contact.<sup>28</sup>

This iterative formalism can be translated into a corresponding capacitance network (Fig. 3). Here we have used the geometric capacitance  $C_{i,i+1}$  between adjacent layers (see Fig. 2). It can be seen that the quantum capacitance of the  $i$ th system is connected in parallel to all systems with a lower index.

We now proceed to use Eqs. (6) and (8) for the interpretation of our capacitance data. It should be pointed out, though, that the derived formalism is of much broader applicability. It could, e.g., be the starting point for a generalization of the capacitive depth profiling method<sup>20</sup> for nonclassical systems.

#### A. Application to the present system

The system under consideration here, with a 2DEG and a quantum dot layer, constitutes the case  $N=2$ .

The capacitance  $C^{(0)} = 4.69$  nF/cm<sup>2</sup> can be measured directly by applying a high negative gate voltage  $U < -2$  V, so that both the 2DEG and the dots are depleted. Note that this depletion characteristic also accounts for any capacitances of

the measurement setup, so that no additional parallel capacitance has to be included in the equations.

Furthermore, the quantum capacitance  $C_{q,1}$  of the 2DEG is well known and independent of gate bias:

$$C_{q,1} = e^2 D_1(E_2) = \frac{e^2 m^*}{\pi \hbar^2}, \quad (9)$$

where  $m^* = 0.067 m_0$  is the effective mass of the 2D electrons. It should be noted that this expression may be violated in the limit of low electron densities. In high-mobility samples the depletion region can even exhibit a *negative* compressibility.<sup>21-23</sup> Here, we neglect this complication because in our low-mobility samples the measured capacitance in this gate voltage region is obscured by resistive effects and these quantum corrections are only a very small effect.

The geometric capacitance  $C_{1,g}$  between gate and the 2DEG can be determined from the growth parameters and from self-consistent calculations.<sup>24</sup> These show that the wave function of the electrons in the 2DEG resides approximately 5 nm away from the Al<sub>x</sub>Ga<sub>1-x</sub>As/GaAs interface. This leads to a total capacitance of  $C^{(1)} = 35.5$  nF/cm<sup>2</sup>, which can be used in the second iteration step:

$$\frac{1}{C^{(2)}} = \frac{1}{C_{2,g}} + \frac{1}{C_{q,2} + \frac{C_{2,g} C^{(1)}}{C_{2,g} - C^{(1)}}}. \quad (10)$$

Here, again, the geometric capacitance  $C_{2,g}$  between gate and dot layer includes a small correction of 2 nm to account for a shift of the wave function away from the nominal GaAs/InAs interface position. Equation (10) can be used to determine the quantum capacitance  $C_{q,2}$  of the dot layer from the measured capacitance  $C^{(2)}$ . This quantum capacitance originates from the inhomogeneously broadened spectrum of the quantum dots, which results in an average density of states  $D_2(E)$  of the dot *ensemble*,

$$C_{q,2} = e^2 D_2(E_F) = \frac{e^2}{n} \sum_{i,k} \delta(E_F - \epsilon_{i,k}), \quad (11)$$

where  $E_F$  is the Fermi energy in the dot layer. The sum takes into account all dots under the gate (total number  $n$ , index  $i$ ) and all energy states in the dots (index  $k$ ). Combining Eqs. (2) and (10) the total capacitance  $C^{(2)}$  can be related to the change of the carrier concentration in the dot layer:

$$C^{(2)} = C^{(1)} + \frac{d\sigma_{dot}}{dU} \left( 1 - \frac{C^{(1)}}{C_{2,g}} \right). \quad (12)$$

Here,  $C^{(2)}$  is the measured capacitance and  $C^{(1)}$  can be determined in the gate bias region, where the dots are depleted but the 2DEG is charged.  $C_{2,g}$  is the geometric capacitance between the dot layer and the gate.

Using Eq. (12), the charge transfer into the dot layer can be calculated from the measured capacitance:

$$\frac{d\sigma_{dot}}{dU} = C_{2,g} \frac{C^{(2)} - C^{(1)}}{C_{2,g} - C^{(1)}}. \quad (13)$$

More practically,  $d\sigma_{dot}$  is expressed in terms of the change in capacitance  $\Delta C = C^{(2)} - C^{(1)}$ , induced by the presence of the

quantum dot layer, and the effective capacitance between the dot layer and the (complex) back contact,  $1/C^{(b,2)}=1/C^{(1)}-1/C_{2,g}$ :

$$\frac{d\sigma_{dot}}{dU} = \Delta C \frac{C^{(b,2)}}{C^{(1)}}. \quad (14)$$

The charging characteristic of the dot layer can thus be determined by taking the amplitude of the dot charging peaks with respect to the background capacitance of the 2DEG, multiplied by a corrective factor  $C^{(b,2)}/C^{(1)}$ . In the simple case of a dot layer inserted between the gate and a *metallic* back contact, this corrective factor corresponds to the so-called lever arm, frequently used for the evaluation of quantum dot CV spectra.<sup>4-6,14,15</sup> For our heterostructure we derive an *effective* lever arm of 8.08 by including the different dielectric constants, the nature of the back contact, and the depletion characteristic.

A direct consequence of Eq. (14) is, that only a small fraction of the charge in the dots reveals itself as an increase in the capacitance. More pronounced is the influence of the dots on the charging characteristic of the 2DEG,

$$\frac{d\sigma_{2d}}{dU} = \frac{d\sigma_g}{dU} - \frac{d\sigma_{b,1}}{dU} - \frac{d\sigma_{dot}}{dU}, \quad (15)$$

which, with the above formalism, can also be determined from capacitance data. However, as we will show in the following, it is not only possible, but can actually be advantageous, to take the inverse route and perform quantum dot spectroscopy through detailed measurements of the charging characteristics of the 2D layer. If  $d\sigma_{2d}$  is known, for example from Hall measurements, the quantum capacitance of the dot layer can be calculated:

$$C_{q,2} = C_{2,g} C^{(b,2)} \left( \frac{d\sigma_{b,2}}{dU} \right)^{-1} - C_{2,g} - C^{(b,2)}. \quad (16)$$

Here, the charge  $\sigma_{b,2}$  accounts for the total number of carriers in the structure apart from the quantum dots and can be derived from  $\sigma_{2D}$  [see Eq. (2)]:

$$d\sigma_{b,2} = d\sigma_{2d} + d\sigma_{b,1} = \left( 1 + \frac{C^{(b,1)}}{C_{q,1}} \right) d\sigma_{2d}. \quad (17)$$

In our experiment the 2D density of states is very high, so that the 2DEG almost perfectly screens the remaining part of the heterostructure and the correction introduced by  $d\sigma_{b,1}$  is only of the order of 0.1%, which is approximately the resolution the experiment.

#### IV. EXPERIMENTAL RESULTS

Figure 4 shows a capacitance trace of a large area gate ( $6.4 \times 10^{-3} \text{ cm}^2$ ).

At very low gate voltages ( $< -1.4 \text{ V}$ ), the 2DEG is depleted and only the residual capacitance of the sample and the measurement setup is observed ( $C^{(0)}$ ). Around  $-1.4 \text{ V}$  the 2DEG is charged with electrons and becomes the active back electrode once its conductivity is sufficiently high. Since the two-dimensional density of states is constant this results in

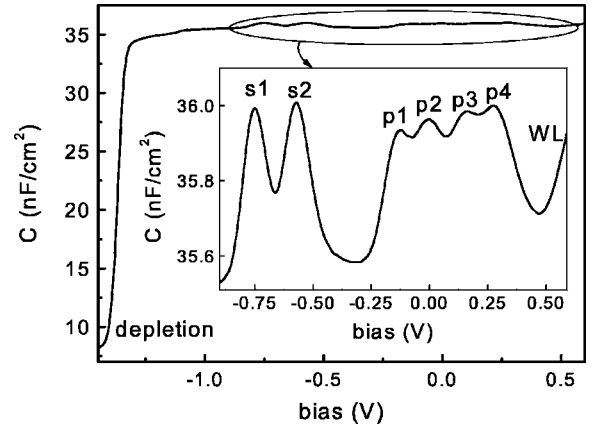


FIG. 4. Capacitance of a heterostructure containing a 2D and a 0D electron system. On top of the almost constant background, originating from the 2DEG, six individual charging peaks of the quantum dots are observed. The inset shows in more detail the bias range where the quantum dots are successively charged.

an almost constant capacitance over the whole voltage range; the small increase in capacitance can be attributed to a shift of the actual position of the 2D wave function. On top of this background, six dot-induced charging peaks are discernible (inset of Fig 4). Finally, at  $U=0.5 \text{ V}$  tunneling into the InAs wetting layer leads to a steep increase in capacitance.

Each of the six charging peaks corresponds to the adding of an individual electron per dot. The first two electrons occupy the  $s$  shell ( $\ell=0$ ) of the quantum dots; the group of four peaks at higher gate voltages represents the occupation of the  $p$  shell ( $\ell=\pm 1$ ). In the commonly used model,<sup>25,26</sup> the confinement perpendicular to the growth direction is described by a 2D harmonic potential and one obtains the observed twofold degeneracy for the  $s$  shell and a fourfold degeneracy for the  $p$  shell.

Since the charging of a quantum dot with an additional electron requires extra energy due to the Coulomb blocking, in the CV spectra these degeneracies are lifted and the charging of single electrons per dot can be observed. This Coulomb energy depends on the actual occupation number of the quantum dot and is especially large for the  $s$  electrons, which are therefore better resolved than the  $p$  shell.

From these capacitance data both carrier concentrations and the quantum capacity of the dot system can be calculated using the above formalism. While the charging of the quantum dots leads to a small increase in capacitance, the effective lever arm  $C^{(b,1)}/C^{(1)}=8.08$  induces a correspondingly larger change in  $dn_{2D}/dU$  and, in the opposite direction, in  $dn_{dot}/dU$  (Fig. 5). As can be seen from the inset of Fig. 5, our model enables us to precisely determine the charging state of both quantum systems for each gate voltage position. With this information we derive a value of  $3.75 \times 10^9 \text{ cm}^{-2}$  for the dot density, which is well below the value determined from atomic force microscopy pictures of dots grown on the sample surface ( $7 \times 10^9 \text{ cm}^{-2}$ ).

To test the validity of our model and to implement a different way to observe the quantum dot charging process, we performed precise Hall measurements to detect  $n_{2D}$ . Previously this has not been possible because of the nature of the

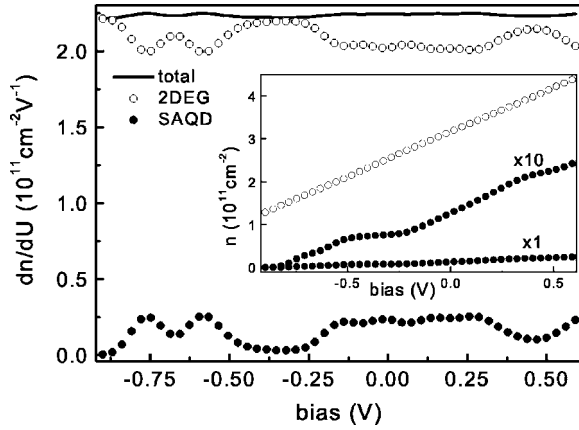


FIG. 5. Change of the number of electrons for both quantum systems. The inset shows the absolute values.

commonly used 3D back contact. Surprisingly, the influence of the (vertical) quantum dot charging process is even more pronounced in these lateral experiments (Fig. 6). Figure 6(a) shows the 2D carrier concentrations determined in both experiments (Hall and CV). Since resistive effects obscure the capacitance data in the region close to the depletion bias it is

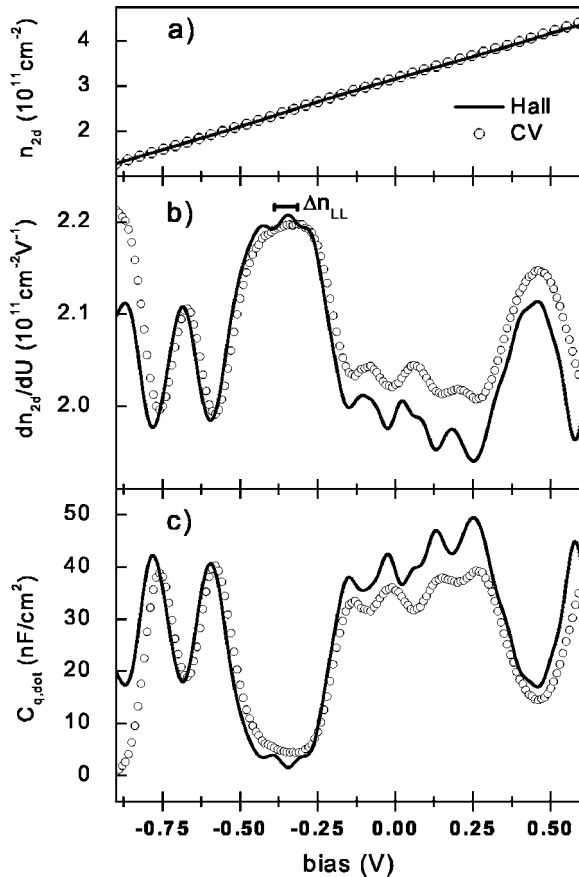


FIG. 6. Carrier concentration (a), the derivative  $dn_{2D}/dU_g$  (b), and quantum capacitance of the dot layer (c), determined by CV (circles) and Hall measurements (solid lines). In (b)  $\Delta n_{LL}$  corresponds to a gate voltage difference which completely fills a Landau level at  $B=0.3$  T.

difficult to derive precise absolute values for  $n_{2D}$  from such capacitance measurements. We have therefore normalized the capacitance data at a gate bias of  $-0.9$  V so that the value of  $n_{2D}$  determined via the Hall experiment is reproduced at this starting point prior to the occupation of the quantum dots. With this correction, Hall measurements [solid lines in Fig. 6(a)] and the values determined from capacitance data [open circles in Fig. 6(a)] are in very good agreement over the whole voltage range. However, for positive gate voltages the Hall measurement shows a slightly slower increase. This can be observed in more detail in Fig. 6(b), where, especially in the region of the  $p$  shell, the Hall measurement shows a more prominent influence of the quantum dots and therefore smaller values of  $dn_{2D}$ . It is surprising that in this voltage region the Hall measurement exhibits a slightly better resolution of the  $p$ -shell electrons in conjunction with a higher peak-to-valley ratio.

In both experiments the reduction of  $dn_{2D}$  due to the charging of the wetting layer around  $0.5$  V can be observed. Once the electron concentration is high enough such that the wetting layer becomes conducting it acts as a second 2DEG, the Hall voltage decreases, and an apparent increase of  $dn_{2D}$  is observed in the Hall experiment ( $0.57$  V).

Another additional feature of the Hall experiments are the small kinks which are most pronounced between the  $s$  and  $p$  shells and at the center of the  $p$  shell. We attribute these features to the beginning of the formation of quantum Hall plateaus, which is in agreement with the gate voltage difference necessary to change  $n_{2D}$  by  $\Delta n_{LL}$  [see Fig. 6(b)], which completely fills the next Landau level at  $B=0.3$  T. These kinks can in principle be suppressed if a smaller magnetic field is applied when measuring the Hall voltage, which, however, reduces the signal-to-noise ratio.

As a final step the quantum capacitance of the dot layer can be calculated from the Hall data. Similar to capacitance measurements, the geometric capacitances are used to deduce the quantum capacitance  $C_{q,dot}$  and the corresponding density of states  $D_2=C_{q,dot}/e^2$  of the dot layer [Eq. (17)]. The quantum capacitance thus derived of the dot layer in comparison to the capacitance data is displayed in Fig. 6(c). Again, both experiments result in very similar traces, which is a good indication of the applicability of our capacitance model in this system. In fact, the measurement of  $n_{2D}$  enables us to determine the characteristics of the quantum dot ensemble with at least the same accuracy as can be expected from typical capacitance data. For example, we calculated a value of  $4 \times 10^9$   $\text{cm}^{-2}$  for the areal dot density, which is a significant improvement over the result determined from CV spectroscopy.

Additionally, we employed both experiments to determine the Coulomb energies for the first six quantum dot electrons (Table I). We find a very good agreement between both methods and also with similar values from previous studies of InAs quantum dots.<sup>14,15</sup> Using the formalism of Warburton *et al.*<sup>15</sup> we can also estimate the quantization energy  $\hbar\omega_c$  to be approximately  $50$  meV, which is in good agreement with previous reports.<sup>5,14,15</sup>

In summary, we have developed a general model to analyze capacitance and Hall measurements of samples with multiple embedded quantum systems with a reduced density

TABLE I. Coulomb energies determined via Hall measurements and CV spectroscopy. The values marked with an asterisk were calculated assuming a quantization energy of 50 meV, which is a typical value for the growth parameters used here and supported by magnetic-field-dependent capacitance measurements (not shown here).

Electrons	$\Delta E_{Hall}$ (meV)	$\Delta E_{CV}$ (meV)
$s_1$ - $s_2$	23.93	21.66
$s_2$ - $p_1$	7.23*	7.61*
$p_1$ - $p_2$	16.88	16.01
$p_2$ - $p_3$	20.96	19.59
$p_3$ - $p_4$	15.89	16.02

of states. The iterative formalism was applied to a heterostructure containing a 2DEG and a layer of self assembled InAs quantum dots and allowed us to determine the carrier concentrations of both systems over the whole voltage range. Similarly, the formalism was employed to extract the quan-

tum capacitance of the dot layer from a very sensitive Hall measurement. While both complementary methods can be used for quantum dot spectroscopy it is surprising that the rather indirect in-plane Hall measurement gives a slightly better peak-to-valley ratio and also a better approximation of the number of simultaneously charged quantum dots. Also, the possibility to use a dc setup to measure  $n_{2D}$  makes a whole class of heterostructures with very large tunneling resistances accessible, where CV spectroscopy is not practical. We note, however, that such Hall measurements are only possible for nonquantizing magnetic fields.

#### ACKNOWLEDGMENTS

The authors thank J. H. Davies for valuable discussions. M.R. gratefully acknowledges financial support under Grant No. 01BM461 by the German Bundesministerium für Bildung und Forschung. Moreover, financial support from the BMBF under Grant No. 01BM451 and from Deutsche Forschungsgemeinschaft (DFG) under Grant No. GRK384 is gratefully acknowledged.

\*Electronic address: axel.lorke@uni-duisburg.de

<sup>1</sup>D. Bimberg, M. Grundmann, and G. Abstreiter, *Quantum Dot Heterostructures* (Wiley, Chichester, U.K., 1998).

<sup>2</sup>P. M. Petroff, A. Lorke, and A. Imamoglu, *Phys. Today* **54**(5), 46 (2001).

<sup>3</sup>S. M. Reimann and M. Manninen, *Rev. Mod. Phys.* **74**, 1283 (2002).

<sup>4</sup>G. Medeiros-Ribeiro, F. G. Pikus, P. M. Petroff, and A. L. Efros, *Phys. Rev. B* **55**, 1568 (1997).

<sup>5</sup>B. T. Miller, W. Hansen, S. Manus, R. J. Luyken, A. Lorke, J. P. Kotthaus, S. Huan, G. Medeiros-Ribeiro, and P. M. Petroff, *Phys. Rev. B* **56**, 6764 (1997).

<sup>6</sup>R. J. Luyken, A. Lorke, A. O. Govorov, J. P. Kotthaus, G. Medeiros-Ribeiro, and P. M. Petroff, *Appl. Phys. Lett.* **74**, 2486 (1999).

<sup>7</sup>O. Wibbelhoff, A. Lorke, D. Reuter, and A. D. Wieck, *Appl. Phys. Lett.* **86**, 026808 (2005).

<sup>8</sup>H. Sakaki, G. Yusa, T. Someya, Y. Ohno, T. Noda, H. Akiyama, Y. Kadoya, and H. Noge, *Appl. Phys. Lett.* **67**, 3444 (1995).

<sup>9</sup>G. H. Kim, D. A. Ritchie, M. Pepper, G. D. Lian, J. Yuan, and L. M. Brown, *Appl. Phys. Lett.* **73**, 2468 (1998).

<sup>10</sup>G. H. Kim, J. T. Nicholls, S. I. Khondaker, I. Farrer, and D. A. Ritchie, *Phys. Rev. B* **61**, 10910 (2000).

<sup>11</sup>E. Ribeiro, E. Müller, T. Heinzel, H. Auderset, K. Ensslin, G. Medeiros-Ribeiro, and P. M. Petroff, *Phys. Rev. B* **58**, 1506 (1998).

<sup>12</sup>E. Ribeiro, R. D. Jäggi, T. Heinzel, K. Ensslin, G. Medeiros-Ribeiro, and P. M. Petroff, *Phys. Rev. Lett.* **82**, 996 (1999).

<sup>13</sup>A. A. Zhukov, C. Weichsel, S. Beyer, S. Schnüll, C. Heyn, and

W. Hansen, *Phys. Rev. B* **67**, 125310 (2003).

<sup>14</sup>M. Fricke, A. Lorke, J. P. Kotthaus, G. Medeiros-Ribeiro, and P. M. Petroff, *Europhys. Lett.* **36**, 197 (1996).

<sup>15</sup>R. J. Warburton, B. T. Miller, C. S. Dürr, C. Bödefeld, K. Karrai, J. P. Kotthaus, G. Medeiros-Ribeiro, P. M. Petroff, and S. Huan, *Phys. Rev. B* **58**, 16221 (1998).

<sup>16</sup>T. P. Smith, B. B. Goldberg, P. J. Stiles, and M. Heiblum, *Phys. Rev. B* **32**, 2696 (1985).

<sup>17</sup>T. P. Smith III, W. I. Wang, and P. J. Stiles, *Phys. Rev. B* **34**, R2995 (1986).

<sup>18</sup>S. Luryi, *Appl. Phys. Lett.* **52**, 501 (1988).

<sup>19</sup>M. Büttiker, *J. Phys.: Condens. Matter* **5**, 9361 (1993).

<sup>20</sup>D. P. Kennedy, P. C. Murley, and W. Kleinfelder, *IBM J. Res. Dev.* **12**, 399 (1968).

<sup>21</sup>J. P. Eisenstein, L. N. Pfeiffer, and K. W. West, *Phys. Rev. Lett.* **68**, 674 (1992).

<sup>22</sup>J. P. Eisenstein, L. N. Pfeiffer, and K. W. West, *Phys. Rev. B* **50**, 1760 (1994).

<sup>23</sup>L. Calmels and A. Gold, *Phys. Rev. B* **52**, 10841 (1995).

<sup>24</sup>Greg Snider, Poisson solver Dept. of Electrical Engineering, University of Notre Dame, Notre Dame, IN 46556, USA. Electronic address: snider.7@nd.edu

<sup>25</sup>V. Fock, *Z. Phys.* **47**, 446 (1928).

<sup>26</sup>C. G. Darwin, *Proc. Cambridge Philos. Soc.* **27**, 86 (1930).

<sup>27</sup>All capacitances are normalized to the gate area (F/m<sup>2</sup>).

<sup>28</sup>For a treatment of a system which is not in equilibrium, so that its response has both capacitive and resistive contributions, see, e.g., Ref. 10.